A model for quorum-sensing mediated stochastic biofilm nucleation

Supplementary Information

Patrick Sinclair, Chris A. Brackley, Martín Carballo-Pacheco and Rosalind J. Allen

FIXED POINTS OF THE DETERMINISTIC MODEL

The deterministic version of our model is described by the following set of M ordinary different equations representing M microhabitats [Eq. (1) in the main text]

$$\frac{dN_i}{dt} = gN_i\left(1-\frac{N_i}{K}\right) + \frac{r_{\rm mig}}{2}\left[(1-\delta_{iM})N_{i+1} + (1-\delta_{i1})N_{i-1} - (2-\delta_{i1}-\delta_{iM})N_i\right] + \delta_{iM}\left[r_{\rm im} - N_i r_{\rm det}\right], \quad \text{(S1)}$$

where N_i is the number of bacteria in microhabitat i ($i = 1, 2, \ldots, M$) and δ_{ij} is the Kronecker delta ($\delta_{ij} = 1$ if $i = j$ and 0 otherwise). We couple this to the dynamics of increasing numbers of microhabitats where we start with $M = 1$ at $t = 0$ and increase M by 1 whenever $N_M = N^*$ (where $N^* = \rho^* a\,\delta z$ is the biofilm formation threshold, with ρ^* being a threshold bacterial density for the transition to the biofilm state). The first term in Eq. (S1) represents logistic growth, with a maximal rate g, with subsequent terms describing migration, immigration and detachment. Here, we discuss in more detail the fixed points of these equations.

A single microhabitat

To understand the dynamics in the very early stages of biofilm formation we consider the case of a single microhabitat ($M = 1$),

$$\frac{dN_1}{dt} = gN_1\left(1-\frac{N_1}{K}\right) + r_{\rm im} - N_1 r_{\rm det}, \quad \text{(S2)}$$

and obtain the steady state by setting $dN_1/dt = 0$. Solving the resulting quadratic gives the fixed points

$$N^{\pm}_{1,M=1} = \frac{K}{2}\left(1-\frac{r_{\rm det}}{g}\right)\left[1 \pm \left(1 + \frac{r_{\rm im}}{gK}\frac{4}{\left(1-\frac{r_{\rm det}}{g}\right)^2}\right)^{1/2}\right], \quad \text{(S3)}$$

where we have included $M = 1$ in the subscript to indicate that these solutions only refer to the case of a single microhabitat. The nature of these fixed points can be inferred from a plot of $f_{1,M=1}(N_1) \equiv dN_1/dt$: the larger fixed point is stable, while the smaller one is unstable (hereon we use $N^{\rm fp}_{1,M=1}$ to refer to the stable fixed point, *i.e.*, the one with with the largest value). The equations can be made dimensionless by considering the ratio N_1/K and the dimensionless parameters $r_{\rm det}/g$ and $r_{\rm im}/(Kg)$. Figure S1 shows how $N^{\rm fp}_{1,M=1}$ depends on these parameters.

We note that if $r_{\rm det}/g = r_{\rm im}/(Kg)$ (or equivalently, $r_{\rm det}K/r_{\rm im} = 1$), then $N^{\rm fp}_{1,M=1}/K = 1$. This points to the existence of two regimes: if $r_{\rm det}K/r_{\rm im} < 1$ then the fixed point is greater than the carrying capacity, *i.e.* $N^{\rm fp}_{1,M=1}/K > 1$, since

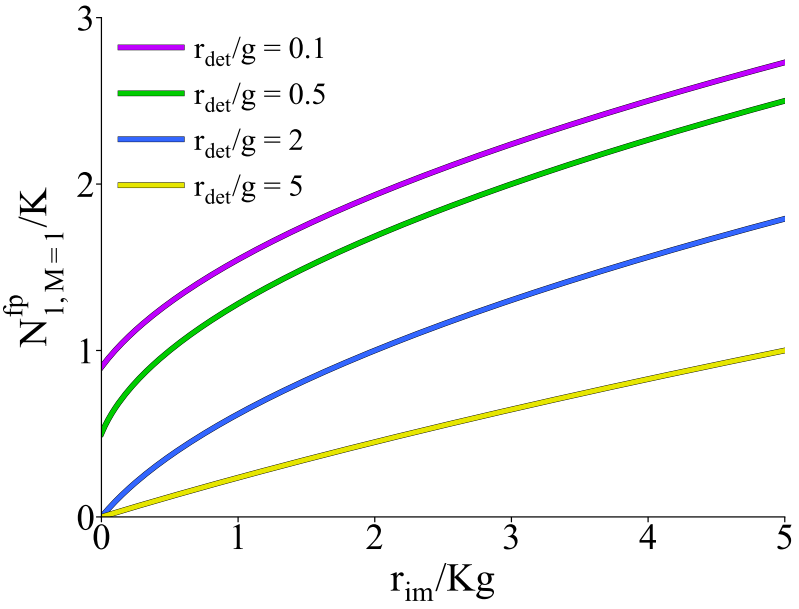

FIG. S1. Value of the largest fixed point for the single microhabitat case $N^{\rm fp}_{1,M=1}$, as given by Eq. (S3), scaled by the carrying capacity K and plotted as a function of the dimensionless parameter $r_{\rm im}/gK$, for various values of the dimensionless parameter $r_{\rm det}/g$.

growth is augmented by immigration. In contrast, if $r_{\rm det}K/r_{\rm im} > 1$ then instead the fixed point is less than the carrying capacity, *i.e.* $N^{\rm fp}_{1,M=1}/K < 1$, since the population is depleted by detachment from the surface microhabitat.

Two further parameter regimes emerge when we consider the relative size of the stable fixed point and the biofilm threshold N^*. For an initial condition $M = 1$ and $N_1(t = 0) = 0$, if $N^{\rm fp}_{1,M=1} < N^*$ the system will grow only until $N_1(t) \to N^{\rm fp}_{1,M=1}$. Thus the population reaches a steady state, but the biofilm will never fully become established. However, if $N^{\rm fp}_{1,M=1} > N^*$, the system will grow until $N_1(t) = N^*$, at which point the first microhabitat will transition to the biofilm state, and a second microhabitat will be generated. These are the regimes separated by the solid line in Fig. 2(a) in the main text; note that this line always goes through the point $N^*/K = 1$, $r_{\rm det}K/r_{\rm im} = 1$, but otherwise depends on the dimensionless ratios $r_{\rm im}/gK$ and $r_{\rm det}/g$.

Two microhabitats

For $M = 2$ microhabitats, the system is governed by two equations

$$\frac{dN_1}{dt} = f_1(N_1, N_2), \qquad \frac{dN_2}{dt} = f_2(N_1, N_2),$$

where

$$f_1(N_1, N_2) = gN_1\left(1 - \frac{N_1}{K}\right) + \frac{r_{\rm mig}}{2}\left[N_2 - N_1\right], \tag{S4}$$

$$f_2(N_1, N_2) = gN_2\left(1 - \frac{N_2}{K}\right) + \frac{r_{\rm mig}}{2}\left[N_1 - N_2\right] + \left[r_{\rm im} - N_2 r_{\rm det}\right]. \tag{S5}$$

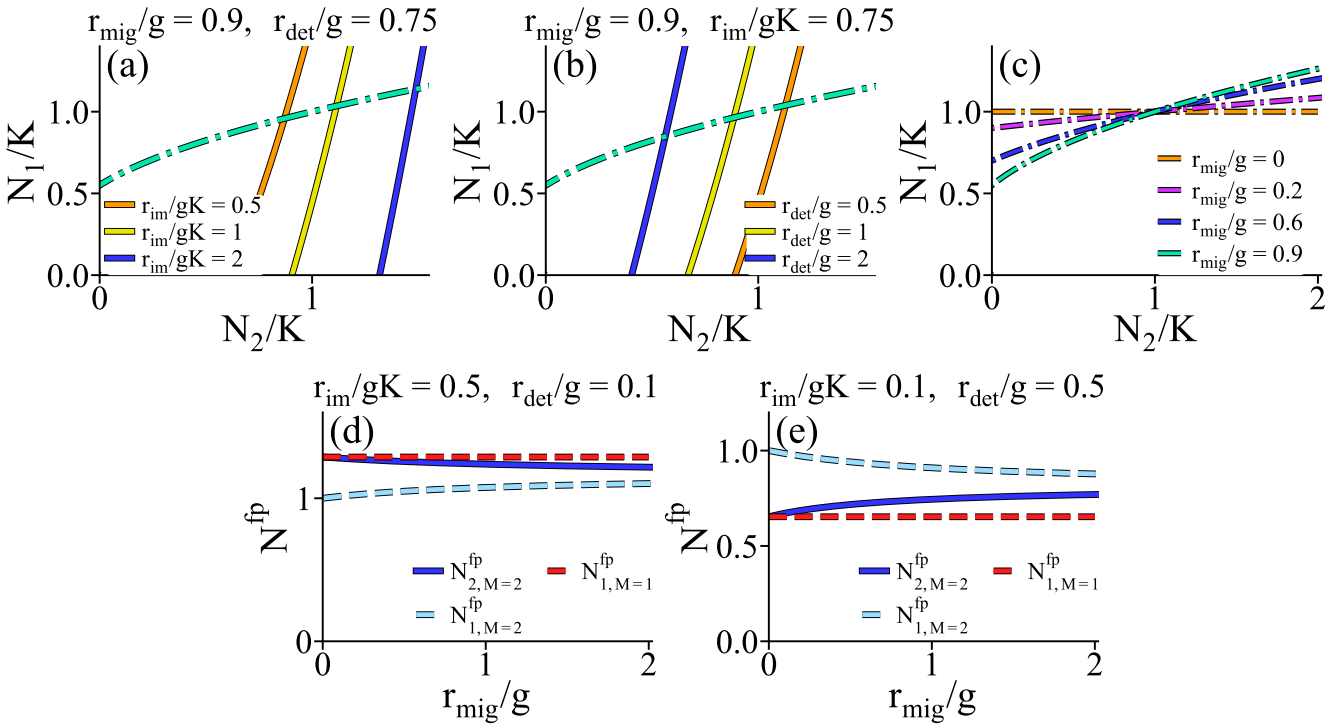

FIG. S2. (a) Curves in the (N_1, N_2) plane corresponding to $f_1(N_1, N_2) = 0$ [dot-dash line, Eq. (S4)] and $f_2(N_1, N_2) = 0$ [solid lines, Eq. (S5)], plotted for different values of $r_{\rm im}$. The intersection of these curves gives the fixed point (both equations equal zero); there is a second intersection which has a negative value of N_1 or N_2 (and that fixed point is unstable). Note that $f_1(N_1, N_2)$ is independent of $r_{\rm im}$ and $r_{\rm det}$. Other parameters are $r_{\rm det}/g = 0.75$, $r_{\rm mig}/g = 0.9$, $g = 1$ and $K = 1$. (b) Similar plot showing $f_1(N_1, N_2) = 0$ (dot-dash line) and $f_2(N_1, N_2) = 0$ (solid), but for different values of $r_{\rm det}$. Here $r_{\rm im}/gK = 0.75$ and the other parameters are as in panel (a). (c) The curve corresponding to $f_{1,M=2}(N_1, N_2) = 0$ plotted for different values of $r_{\rm mig}/g$. For $r_{\rm mig} = 0$ this gives a horizontal line, indicating that the equations for N_1 and N_2 become decoupled. (d) Fixed point values for the two-microhabitat system (blue lines) as a function of $r_{\rm mig}$ for the case $r_{\rm det}K/r_{\rm im} < 1$ (found numerically from the intersections of curves as in panels (a)-(b). The red-dashed line indicates the fixed point value for the corresponding one-microhabitat case [which is independent of $r_{\rm mig}$; Eq. (S3)]. Note that $N^{\rm fp}_{1,M=1} \geq N^{\rm fp}_{2,M=2}$. (e) A similar plot for the case where $r_{\rm det}K/r_{\rm im} > 1$. Here $N^{\rm fp}_{1,M=1} \leq N^{\rm fp}_{2,M=2}$.

Again we consider the fixed points ($dN_1/dt = 0, dN_2/dt = 0$), which now leads to two non-linear equations coupled through the migration terms. For a given set of parameters, these can be inspected graphically as the intersection of the two curves in the (N_1, N_2) plane corresponding to $f_1(N_1, N_2) = 0$ and $f_2(N_1, N_2) = 0$ [Figs. S2(a,b)], or they can be solved numerically. It can be inferred that the negative (or zero) fixed point is unstable in favour of the positive one (which we denote $N^{\rm fp}_{1,M=2}, N^{\rm fp}_{2,M=2}$). As before we have the two regimes depending on the value of $r_{\rm det}K/r_{\rm im}$; the values of the fixed points decrease as the ratio $r_{\rm det}K/r_{\rm im}$ increases.

As shown in Fig. S2(c), if $r_{\rm mig} = 0$ then the population dynamics in the two microhabitats are decoupled from each other, such that $N^{\rm fp}_{1,M=2}/K = 1$ and $N^{\rm fp}_{2,M=2} = N^{\rm fp}_{1,M=1}$ (the outermost habitat behaves exactly as the $M = 1$ case). For $r_{\rm mig} > 0$ the behavior depends on the ratio $r_{\rm det}K/r_{\rm im}$, with $N^{\rm fp}_{2,M=2}$ either increasing or decreasing with $r_{\rm mig}$ [Figs. S2(d,e)]. As noted in the main text, for the immigration-dominated regime, $r_{\rm det}K/r_{\rm im} < 1$, when $r_{\rm mig} > 0$ we have $N^{\rm fp}_{2,M=2} < N^{\rm fp}_{1,M=1}$ [compare red dashed and blue solid lines in Fig. S2(d)]. This means that choosing N^* such that $N^{\rm fp}_{2,M=2} < N^* < N^{\rm fp}_{1,M=1}$ gives a system which will grow to generate a second microhabitat, but will then reach

steady state before N_2 grows above N^*, *i.e.*, it will fail to generate a third microhabitat.

Together this leads to the surprising result that a population whose growth is immigration-dominated can reach a steady state population size with two microhabitats that does not grow any further (region between the dashed and solid lines in Fig. 2 in the main text). We note however that this requires a biofilm formation threshold larger than the carrying capacity ($N^* > K$), i.e., a case where the environment cannot sustain a large enough population to trigger biofilm formation. A detachment-limited population will either never fill the first microhabitat ($N^{\rm fp}_{1,M=1} < N^*$), or will grow indefinitely after transitioning to a biofilm state ($N^{\rm fp}_{1,M=1} > N^*$; in this latter case, the inner microhabitats feed the outer ones, boosting the steady state population size).

Further microhabitats

For the case of three or more microhabitats, determining the fixed points amounts to simultaneously solving a set of three or more non-linear equations. Nevertheless, one can again consider the $r_{\rm mig} = 0$ case where the equations decouple, such that the internal microhabitats have a fixed point $N^{\rm fp}_{i<M} = K$ while the outermost microhabitat behaves according to Eq. (S3). For non-zero migration rate, one might imagine that, as with the case of two microhabitats, increasing $r_{\rm mig}$ will lead to an increase or a decrease of the fixed point value depending on the ratio $r_{\rm im}/Kr_{\rm det}$. This can be confirmed by direct numerical solution of a system with a fixed number of equations [i.e., solving Eqs. (S1) with fixed M]; numerical results are shown in Fig. 2(b) in the main text. The value of $N^{\rm fp}_M$ initially depends on M, but then plateaus at large M. For the case of $r_{\rm det}K/r_{\rm im} < 1$ (the population is driven by growth and immigration) the value of $N^{\rm fp}_M$ *decreases* with increasing M (grey points in Fig. 2(b) in the main text). There is a very small range of possible N^* values where $N^{\rm fp}_{4,M=4} < N^* < N^{\rm fp}_{3,M=3}$, where the biofilm would grow to the third microhabitat before halting. This continues for larger M, with an ever decreasing range of possible N^* values.

PARAMETER DEPENDENCE OF THE DETERMINISTIC MODEL

Focussing on the parameter regimes where biofilm growth continues indefinitely, we solved Eqs. (S1) numerically to determine how the different parameters affect biofilm growth. To determine the rate of biofilm growth, we computed the value μ, defined as

$$\mu = \left\langle \frac{dN_{\rm tot}}{dt} \right\rangle, \tag{S6}$$

where $N_{\rm tot} = \sum_{i=1}^{M} N_i$ and the angle brackets indicate that the growth rate is averaged along the growth trajectory (since in our model growth trajectories are 'bumpy' due to the slowing as the population approaches its steady state value in each microhabitat; see for example Fig. 2(c) in the main text). In practice, the value of μ was obtained from a linear fit to $N_{\rm tot}(t)$ found by numerically solving the equations up to $gt = 1 \times 10^4$ (which for parameters exhibiting growth led to generation of at least 14 microhabitats). We also determined the waiting time before the transition to the biofilm state in the first microhabitat, which we denote t_1.

Figure S3 shows how μ and t_1 depend on the various parameters. As expected, μ grows with $r_{\rm im}$, and reduces with $r_{\rm det}$ (while t_1 shows the opposite dependence). Interestingly, μ shows a step increase from zero as $r_{\rm im}$ increases, before rising more slowly (similarly $t_1 \to \infty$ discontinuously as $r_{\rm im}$ is decreased through the transition). Varying the

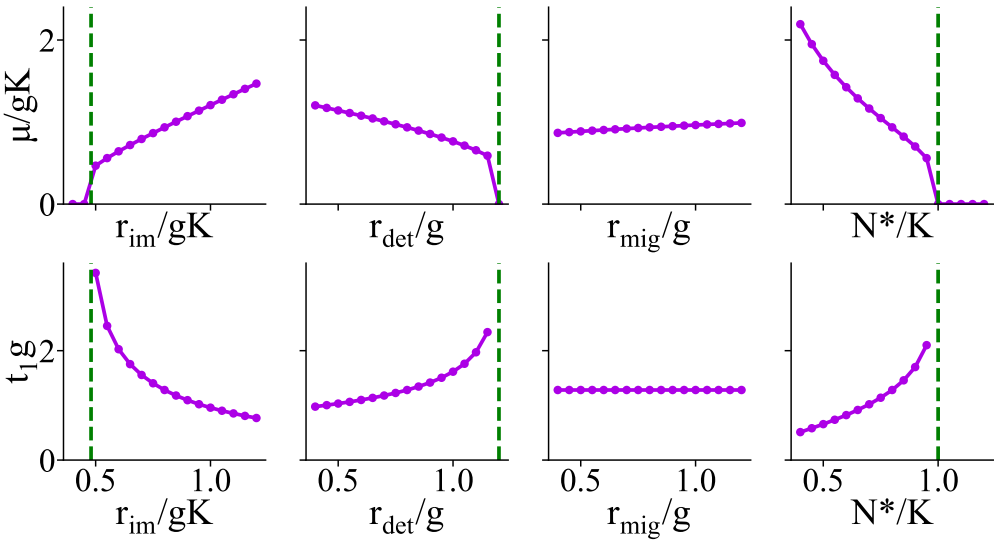

FIG. S3. Plots showing (from left to right in each row) the effect of varying the parameters r_{im}/gK, r_{det}/g, r_{mig}/g, and N^*/K. Values of these dimensionless ratios are set to 0.8 when not being varied, and we fix $g = 1$, $K = 1$. Top row plots show the mean biofilm growth rate μ, as defined in Eq. (S6). Bottom row plots show the time taken to reach the biofilm threshold N^* in the first microhabitat t_1. Points are obtained from numerical integration of Eqs. (S1) up to a total time equivalent to $tg = 1 \times 10^4$; connecting lines are drawn as a guide to the eye. The green vertical dashed lines show the deterministic prediction for the boundary between biofilm formation and non-formation (i.e. the parameter values beyond which the first microhabitat does not reach the population density threshold for the biofilm transition).

migration rate has a comparatively small effect on μ and t_1, but varying N^* has a larger effect, and also leads to a discontinuous change at the transition.

STOCHASTIC SIMULATION ALGORITHM

Our stochastic simulations use a version of Gillespie's τ-leaping algorithm [1], modified to avoid negative population sizes [2]. Specifically, the timestep is updated dynamically to ensure that negative population sizes do not occur. Although this is a standard algorithm [2], for clarity we outline the steps involved, from the point of view of our system.

At each simulation timestep, each bacterium in the system can undergo one or more of 4 event types. These are (i) replication, at rate r_{rep} given by $r_{\mathrm{rep}} = g\,(1 - N/K)$ for $N < K$, where g is the maximum growth rate of the bacteria, N is the number of bacteria in the microhabitat and K is the microhabitat's "carrying capacity" (see main text); (ii) death at rate $r_{\mathrm{death}} = g\,(1 - N/K)$ for $N > K$, which arises when the logistic term $g\,(1 - N/K)$ is negative (note that this is the only source of death in the system, bacteria do not die if $N < K$); (iii) migration between microhabitats (if the number of microhabitats is > 1) at rate r_{mig}, or at rate $r_{\mathrm{mig}}/2$ if the bacterium is in the outermost or innermost microhabitat; and (iv) detachment at rate r_{det}, if the bacterium is located in the edge microhabitat.

The numbers of events of each type (i)-(iv) to be undergone by each bacterium are randomly assigned at the start of each timestep. Specifically, for each bacterium and each event type, a number is chosen from a Poisson distribution with mean $r \times \tau$, where r is the rate for that event and τ is the duration of the timestep. In order to prevent negative

populations arising, if a bacterium is assigned to undergo more than 1 death, migration or detachment event in a given timestep, then we halve the timestep, $\tau \to \tau/2$ and begin the entire event assignment process again. If this again generates multiple deaths, detachments or migrations for any bacterium, we again halve the timestep and repeat the process [2]. If a bacterium is designated to both replicate and migrate in the same timestep, it will first replicate, then the mother cell will migrate. Likewise, if it is assigned to both replicate and detach, it will first replicate and then the mother cell will detach. We note that this prioritisation of replication over detachment introduces a small bias towards larger population sizes. However, in our simulations the timestep is small enough that microbes are only rarely assigned to both replicate and detach, so this bias is negligible.

Having assigned event numbers for all bacteria and all event types, these events are implemented. For replication, new bacteria are created in the same microhabitat. For migration, the bacterium moves to the right or left at random (unless it is in the outermost or innermost microhabitat). For death or detachment, the bacterium is removed from the system.

Next, to account for immigration at rate $r_{\rm im}$, a number of immigrants is chosen from a Poisson distribution with mean $r_{\rm im} \times \tau$ and these are added to the outermost microhabitat. The time elapsed in the system is then increased by the value of τ.

Finally, we implement the criterion for the transition to the biofilm state, which allows expansion of the system. If, after all updates, the population size in the outermost microhabitat updates exceeds the threshold N^*, we create a new outermost microhabitat. Detachment and immigration events will then only occur in this new outermost microhabitat.

SYSTEM-SIZE DEPENDENCE OF STOCHASTIC SIMULATION RESULTS

To investigate the role of stochastic fluctuations in the transition to biofilm, we tested the effect of increasing the system size, while keeping all other parameters constant. This should suppress the effects of stochastic fluctations. In our system, increasing system size corresponds to increasing the lateral area a which in turn scales the carrying capacity K and threshold population size N^* (which are obtained by considering the population density, and therefore microhabitat volume), and the immigration rate $r_{\rm im}$ (which scales with area).

Fig. S4(a) shows trajectories of total population size (scaled by K) for 100 replicate simulations, with a parameter set in the immigration dominated regime ($r_{\rm det}K/r_{\rm im} < 1$), for which the fixed point $N^{\rm fp}_{1,M=1}$ is slightly smaller than the biofilm threshold population size N^*. Therefore a random population fluctuation is required for the system to reach the biofilm threshold.

Fig. S4(b) shows the results of simulations for the same values of the dimensionless parameters $r_{\rm im}/gK$, $r_{\rm det}/g$, $r_{\rm mig}/g$ and N^*/K, but increasing a (and therefore K, N^* and $r_{\rm im}$) by a factor of 10. In this case none of the 100 simulations reached the population threshold N^*. Even when the duration of the simulations is increased by a factor of 10, as shown in Fig. S4(c), none of the simulated runs form biofilm. Therefore, suppressing the effect of fluctuations by increasing the system size suppresses biofilm formation.

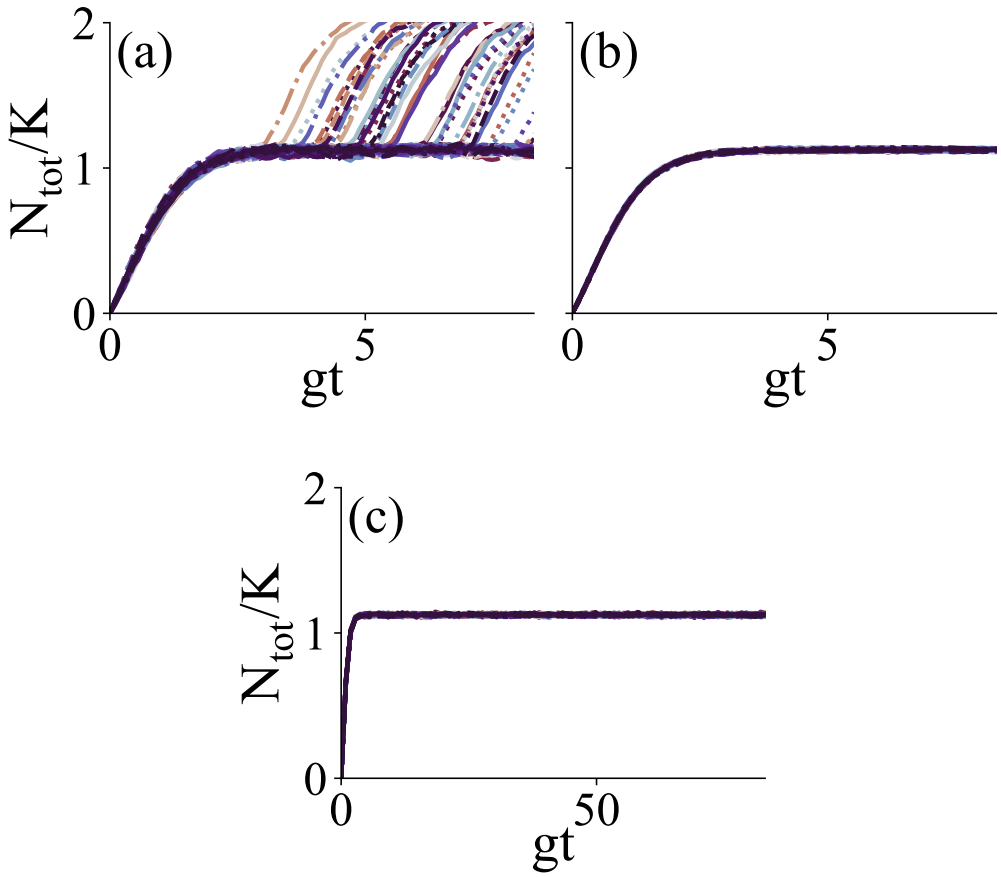

FIG. S4. Effect of increasing the lateral area a of the system (which leads to an increase in the parameters K, N^* and $r_{\rm im}$). The total population size is plotted as a function of time for 100 simulation runs with parameters $r_{\rm im}/gK = 0.7$, $r_{\rm det}/g = 0.5$, $r_{\rm mig}/g = 0.8$ and $N^*/K = 1.17$, with $g = 0.083$. In (a) $K = 1000$, $r_{\rm im}/gK = 0.55$ and $N^*/K = 1.17$, and in (b) and (c) $K = 10000$ $r_{\rm im}/gK = 0.55$ and $N^*/K = 1.17$. Panel (a) therefore corresponds to a system size 10 times smaller than that of panels (b) and (c). Panel (c) differs from (b) only in the duration of the simulation run. In (a) fluctuations drive the formation of a second biofilm in a subset of simulations, whereas in (b) no such transitions to biofilm occur. Even when the duration of the simulation is increased by a factor of 10, as shown in (c), none of the runs are able to establish a biofilm.

COMPARISON BETWEEN STOCHASTIC AND DETERMINISTIC MODEL DYNAMICS

In Fig. 2(c) in the main text we compared population dynamics predictions for our stochastic and deterministic models, for some parameter values. Here, we show equivalent results for a wider range of parameters. In Fig. S5 we consider parameters in the immigration-dominated regime with $N^* > K$,. The dot-dashed pink lines show the deterministic results, and blue lines show corresponding stochastic simulations. For $r_{\rm im}/gK = 0.55$ [Fig. S5(a)], the deterministic and stochastic models show good agreement. However, increasing the immigration rate to $r_{\rm im}/gK = 0.6$ or 0.7 [Figs. S5(b)], leads to a clear discrepancy between the two models, with the stochastic model exhibiting biofilm growth while the deterministic model does not. When $r_{\rm im}/gK = 0.8$ [Fig. S5(c)] the deterministic model predicts formation of a biofilm with finite thickness; this is not observed in the stochastic simulations. Increasing the immigration rate to $r_{\rm im}/gK = 0.9$ results in the stochastic and deterministic models agreeing with one another once again. This illustrates the presence of a region in parameters space where stochastic fluctuations are a driver of biofilm formation.

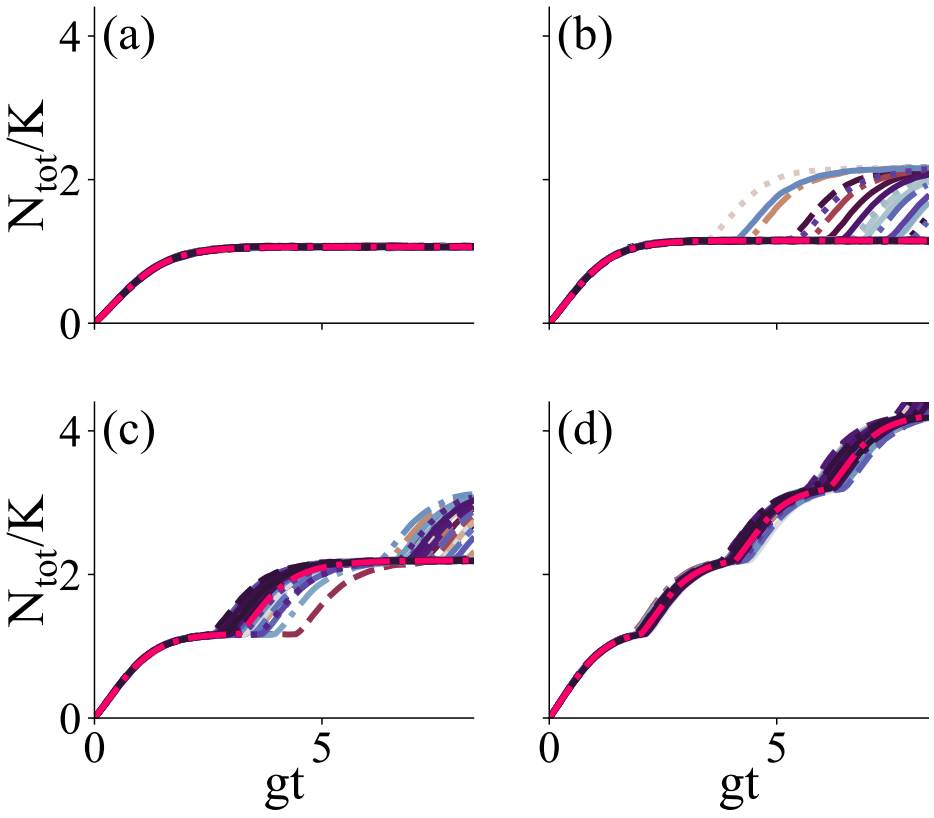

FIG. S5. Comparison between stochastic and deterministic predictions for biofilm growth dynamics, for parameter sets in the immigration-dominated regime. Each plot shows the population size as a function of time for 100 runs of the stochastic model (shades of blue), together with the prediction of the deterministic model (pink dot-dashed line). The value of $r_{\rm im}/gK$ is varied, with (a) $r_{\rm im}/gK = 0.6$, (b) $r_{\rm im}/gK = 0.75$, (c) $r_{\rm im}/gK = 0.8$ and (d) $r_{\rm im}/gK = 0.9$. The other parameters were kept at constant values of $K = 10000$, $g = 0.083$, $r_{\rm det}/g = 0.5$, $r_{\rm mig}/g = 0.8$ and $N^*/K = 1.17$.

Fig. S6 compares stochastic and deterministic predictions for parameters in the detachment-dominated regime. Once again, for a parameter set which has a steady state population close to the biofilm formation threshold, the stochastic model exhibits growth where the deterministic one does not.

FACTORS CONTROLLING THE CARRYING CAPACITY

The carrying capacity K is an important parameter in our model. The carrying capacity, in general, is the maximal bacterial density that can be sustained in a given environment (note that in our model, K is defined as the maximal bacterial number that can be sustained per microhabitat, so it is bacterial density multiplied by microhabitat volume). In a well-mixed system the carrying capacity is usually set by nutrient availability and can be predicted from the concentration of the limiting nutrient, and the growth yield of the bacteria (nutrient consumed per unit biomass produced). In our biofilm model, however, spatial structure makes the situation more complex. Nutrient availability to bacteria close to the surface depends on the rate of diffusion of nutrient from the surrounding environment, versus the rate of consumption by the bacteria. This balance might be very different in different environments, for example in the ocean compared to the rich nutrient media used in the lab. If nutrient abundance is high, the packing density

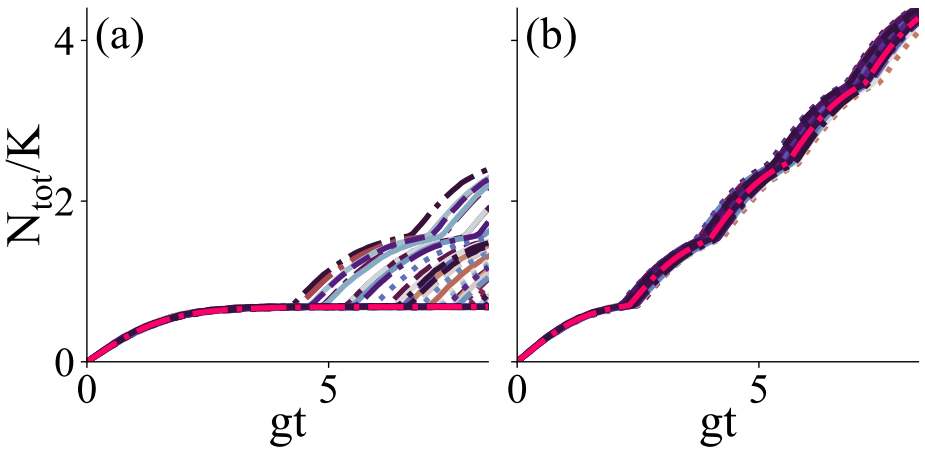

FIG. S6. Comparison between stochastic and deterministic predictions for biofilm growth dynamics, for parameter sets in the detachment-dominated regime. Each plot shows the population size as a function of time for 100 runs of the stochastic model (shades of blue), together with the prediction of the deterministic model (pink dot-dashed line). Parameters are $K = 10000$, $g = 0.083$, $r_{\rm det}/g = 0.9$, $r_{\rm mig}/g = 0.8$ and $N^*/K = 0.7$. The immigration rate was varied: (a) $r_{\rm im}/gK = 0.4$ and (b) $r_{\rm im}/gK = 0.5$.

of bacteria may become limiting, such that the carrying capacity is actually controlled by packing constraints rather than nutrient availability. In principle, the maximal packing density could be calculated from the bacterial size and geometry, but this might be more complex for bacteria that produce capsular material or surface appendages.

[1] D. T. Gillespie, J. Chem. Phys. **115**, 1716 (2001).

[2] Y. Cao, D. T. Gillespie, and L. R. Petzold, J. Chem. Phys. **123**, 054104 (2005).